Dynamic response of a simply supported liquid-crystal elastomer beam under moving illumination

Jun Zhao [1,*] Yiqing Sun,[1] Yuntong Dai,[1] Jing Wu,[2] and Kai Li[1]

[1]*School of Civil Engineering, Anhui Jianzhu University, Hefei, Anhui 230601, China*
[2]*Dongguan University of Technology, Dongguan 523808, China*

Optically responsive liquid crystal elastomer (LCE) devices have thriving potential to flourish in soft robots and microdrives, owing to their advantages of remote controllability, structural simplicity, and no power supply. In terms of illumination-driven modes, most research has focused on the dynamic response of LCE devices under continuous and periodic illumination, while the theoretical study of the dynamic response under moving illumination is limited. In this paper, based on the coupling of LCE and mechanical deformation under moving illumination, the dynamic model of a LCE simply supported beam is built to investigate its dynamic response under moving illumination. The analytical solution of the dynamic response of the LCE beam under moving illumination is derived through the modal superposition method and the Duhamel integration, and the solution is programed and analyzed with MATLAB software. By numerical calculations, the influence of the internal and driving parameters of the structure on the dynamic response of the LCE simply supported beam can be analyzed. The results show that when the moving speed of illumination reaches the first-order critical frequency, the maximum amplitude of the dynamic response at the beam mid-span will reach a peak. Meanwhile, the dynamic response of beam can be improved by increasing the illumination width, increasing the light intensity, increasing the shrinkage coefficient, and reducing the damping coefficient. This work provides theoretical guidance for applying the dynamic response of LCE devices under moving illumination in soft robots, microactuators, energy harvesters, sensors, etc.

I. INTRODUCTION

Soft materials based on liquid crystalline polymers [1–4], composites [5], and electroactive polymers [6,7] have been designed and matured gradually. As one of these, liquid crystal elastomer (LCE) is a smart material combining liquid crystals and polymer networks [8–10]. Its special way of binding molecules gives LCE distinct properties such as orientation, ferroelectricity [11], piezoelectricity, and optical nonlinearity [12]. When exposed to disparate stimuli of electricity [13–16], light [17–20], heat [21–23], magnetism [24], and chemicals [25], the liquid crystal nematic molecules [26] rearrange, causing material deformation. These various modes of stimulation have a wide range of potential applications in both active and passive systems, such as artificial intelligence [27,28], artificial muscles [29–33], nanotechnologies [34,35], the memory of shapes [36,37], actuators and sensors [38,39], stretchable optical devices [40], and so on. However, among all kinds of stimulation, optical stimulation presents unique features, namely, environmental friendliness, precise control, noncontact, and easy access. Optical stimulation has become a more desirable modality in aerospace, machinery, and civil engineering [41–46].

Research on illumination-driven LCE falls into two categories. One is the self-excited response. This response maintains its periodic movement through self-adjustment, which absorbs energy from a constant environment. The other is the forced response that can be adjusted by changing the external environmental parameters. In terms of self-excited response, Liu *et al.* investigated the programmable deformation of LCE plates under illumination [47]. Warner *et al.* found that the cantilever beam forms a saddlelike shape with different curvature symbols in both length and width directions under illumination [48]. Serak *et al.* experimentally confirmed that focused sunlight can induce a rapid and large-amplitude response of illumination-driven LCE cantilever beams [49]. Li and Cai studied the optical response of a LCE cantilever and developed the corresponding mathematical model [50]. Lee *et al.* further experimentally investigated the self-excited response of LCE cantilever beams by adjusting the liquid crystal orientation [51]. Torras *et al.* studied the response characteristics of LCE cantilever beams embedded with nanotubes [52]. Parrany utilized the finite element method to study the large optical response of the LCE cantilever beam [53]. In terms of forced response, Goriely *et al.* converted a liquid crystal elastic rod under illumination into a one-dimensional model and concluded that this model is applicable to a variety of liquid crystal elastic rods subjected to external stimuli [54]. Ahn *et al.* designed bionic functions, such as photodynamic crawling, extrusion, and untethered jumping, for LCE robots [55]. Rogóż *et al.* scanned a moving laser beam, causing a series of deformations within the LCE brake, and realized remote control of the drive as well as large deformation [56]. Rogóż *et al.* combined three-dimensional (3D) laser technology to realize the conjecture of moving illumination to control

*Corresponding author: junzhao@ahjzu.edu.cn

the LCE robots [57]. Guo *et al.* demonstrated a heliotracking device using liquid crystalline actuators. As the light source is moving around the device, the platform tilt follows, always exposing the payload face to the light [58]. Rogóż *et al.* scanned the LCE robot with a laser, causing it to deform and crawl like a caterpillar [59].

In terms of illumination-driven modes, the main focus of most research has been on the dynamic response of LCE devices under constant illumination and periodic illumination [47–55]. Although there is also some applied research on moving illumination [56–59], there are limited theoretical studies on the dynamic response of LCE devices under moving illumination. In view of this, based on the dynamic LCE mode, the current paper analyzes the dynamic response of a LCE simply supported beam through theoretical analysis and numerical calculations, and further studies the influencing factors of the dynamic response of the LCE simply supported beam under moving illumination by adjusting several dimensionless parameters in the system, which guides the study of the influencing parameters of the LCE simply supported beam and the design of illumination and mechanical energy conversion systems.

The paper is organized as follows. In Sec. II, a dynamic model of the LCE simply supported beam under moving illumination is established, and the governing equation and solution method are derived. Section III plots the dynamic response curves of the LCE beam under moving illumination. In Sec. IV, the influence of external parameters and driving parameters on the mid-span response of the LCE beam under moving illumination is analyzed. Conclusions are given in Sec. V.

II. MODEL AND THEORETICAL FORMULATION

To calculate the dynamic response of the LCE simply supported beam under moving illumination, we need first to establish a dynamic model for simulation. Since LCE tends to shrink together with absorbing photons, when the upper surface of the beam is exposed to illumination, the contraction of the upper surface of the beam causes the entire beam body to respond dynamically. In order to qualitatively study the dynamic response of the model, we will establish the dynamic control equation of LCE simply supported beams under moving illumination, and further use modal superposition to obtain the semianalytical solution of the model.

A. Governing equations of illumination-driven response

We first establish the dynamic model of the LCE simply supported beam under moving illumination, as shown in Fig. 1. The LCE simply supported beam is placed horizontally. An illumination of fixed width b, moving at a certain speed v, from the left end to the right end, irradiates on the upper surface of the beam. When the beam is under moving illumination, the shrinkage strain on the upper surface of the beam is significantly greater than that on the lower surface, and thus the beam will show bending deformation. After the illumination moves away, the LCE fiber will return to its original state. Because of inertia, the deflection of each point on the beam is changing dynamically. $W(x, t)$ is used to describe
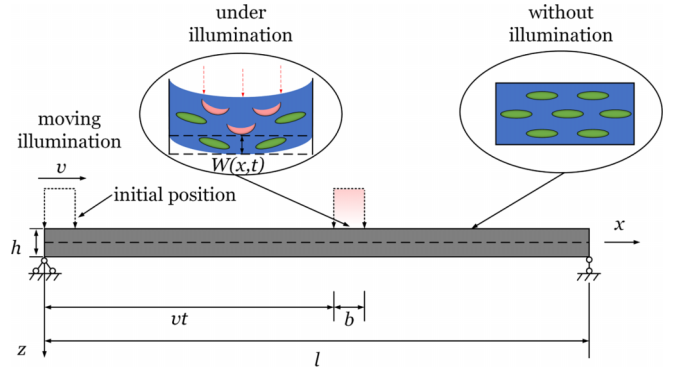

FIG. 1. The dynamic model of the LCE simply supported beam under moving illumination.

the vertical deflection of a certain position of the beam at a certain time.

We assume that the beam height h is much smaller than the beam length l. According to the response theory of continuous beams [60], we can obtain the control equation for the dynamic response of the LCE simply supported beam:

$$\rho_0 \frac{\partial^2 W(x, t)}{\partial t^2} + a \frac{\partial W(x, t)}{\partial t} + B \frac{\partial^4 W(x, t)}{\partial x^2} = -\frac{\partial M(x, t)}{\partial x},$$

$$(1)$$

where a is the damping coefficient [61], $\rho_0 = \rho h$ with ρ being the mass density of the LCE beam, $B = Eh^3/12(1 - \nu^2)$ is the bending stiffness with E and ν being the Young's modulus and Poisson ratio of the beam, and $M(x, t)$ is the bending moment under the moving illumination. We assume that the optically driven shrinkage strain is time independent, so that when there is a sudden change in illumination, the contractile strain changes abruptly. The optical drive moment on the unit interface, $m(x, t)$, can be derived as [48]

$$m(x, t) = \frac{E}{1 - \nu^2} \int_{-h/2}^{h/2} \varepsilon_0(z, t) z dz, \qquad (2)$$

where ε_0 is the bending strain [50], calculated as $\varepsilon_0(z, t) = C_0 \phi(z, t)$, in which C_0 denotes the shrinkage coefficient [62–64] and ϕ refers to the number fraction of the bent *cis* isomers. Neither $\varepsilon_0(z, t)$ nor $\phi(z, t)$ is associated with x; therefore, based on the structural mechanics [65], we can further obtain that

$$\frac{\partial M(x, t)}{\partial x} = m(x, t)[\delta(x - vt) - \delta(x - vt - b)], \qquad (3)$$

where $\delta(x - vt)$ and $\delta(x - vt - b)$ are the Dirac functions. Then we define the following dimensionless parameters: $\bar{W} = W/l$, $\bar{x} = x/l$, $\bar{b} = b/l$, $\bar{t} = t/l^2\sqrt{\rho_0/B}$, $\bar{v} = vl\sqrt{\rho_0/B}$, $\bar{a} = al^2/\sqrt{\rho_0 B}$, and $\bar{M} = M/B$. Then, inserting Eq. (3) into Eq. (1), we can obtain

$$\frac{\partial^2 \bar{W}}{\partial \bar{t}^2} + \bar{a} \frac{\partial \bar{W}(\bar{x}, \bar{t})}{\partial \bar{t}} + \frac{\partial^4 \bar{W}(\bar{x}, \bar{t})}{\partial \bar{x}^4} = \frac{\partial \bar{M}(\bar{x}, \bar{t})}{\partial \bar{x}}, \qquad (4)$$

where $\bar{M}(\bar{x}, \bar{t}) = m(\bar{t})[\delta(\bar{x} - \bar{v}\bar{t}) - \delta\bar{x} - \bar{v}\bar{t} - \bar{b}]$, with

$$m(\bar{t}) = \frac{1}{(1 - \nu^2)h^2} \int_{-h/2}^{h/2} C_0 \varphi(z, t) z dz. \qquad (5)$$

The number fraction of the bent *cis* isomers, $\phi(z, t)$, can be expressed as [66]

$$\phi(z, t) = \phi_0(t) \exp\left(-\frac{h/2 - z}{d_0}\right) \quad \text{for } -h/2 \leqslant z \leqslant h/2, \tag{6}$$

in which d_0 is the penetration depth and $\phi_0(t)$ is the initial number fraction of the *cis* isomers. The latter one can be expressed as [67]

$$\phi_0(t) = \frac{\eta_0 T_0 I_0}{\eta_0 T_0 I_0 + 1}\left[1 - \exp\left(-\frac{t}{T_0}(1 + \eta_0 T_0 I_0)\right)\right], \tag{7}$$

where η_0 represents the light-adsorption constant, T_0 is the thermal relaxation time, and I_0 denotes the light intensity. Since this article assumes that $\frac{t}{T_0} \to +\infty$, the formula can also be expressed as

$$\phi_0(t) = \frac{\eta_0 T_0 I_0}{\eta_0 T_0 I_0 + 1}. \tag{8}$$

In order to simplify the effect on parameter t, we assume that the time for the *cis-trans* isomer conversion is much smaller than the moving time of the illumination we set. Therefore, we ignore the influence of time on the *trans-cis* isomerization and the *cis-trans* isomerization, which can both be represented by Eq. (8).

Substituting Eq. (6) into Eq. (5), we can have

$$m(\bar{t}) = \bar{T}_0 \bar{I}_0 \bar{\phi}_0, \tag{9}$$

where $\bar{I}_0 = 12 I_0 \eta_0 C_0 l^2 \sqrt{\rho_0/B} \bar{d}_0^2[\bar{h}/2\bar{d}_0 - 1 + (1 + \bar{h}/2\bar{d}) \exp(-\bar{h}/\bar{d}_0)]/\bar{h}^3$, $\bar{d}_0 = d_0/l$, $\bar{h} = h/l$, $\bar{T}_0 = T_0/l^2\sqrt{\rho_0/B}$ and $\bar{\phi}_0 = \phi_0/T_0\eta_0 I_0$.

Since the LCE beam is initially stationary, we can list the initial conditions as

$$\bar{W}(\bar{x}, \bar{t} = 0) = 0, \quad \frac{\partial \bar{W}(\bar{x}, \bar{t} = 0)}{\partial \bar{t}} = 0. \tag{10}$$

We can conjecture that the solution to control equation (4) is

$$\bar{W}(\bar{x}, \bar{t}) = \sum_{j=1}^{\infty} q_j(\bar{t}) Y_j(\bar{x}), \tag{11}$$

where $q_j(\bar{t})$ represents the time function of motion law, and $Y_j(\bar{x}) = \sin \beta_j \bar{x}$ is the mode function of the simply supported beam, with modal characteristic value $\beta_j = j\pi$ $(j = 1, 2, 3, \dots)$.

Substituting Eq. (11) into Eq. (4), we can obtain [68]

$$\frac{d^2 q_j(\bar{t})}{d\bar{t}^2} + 2\zeta_j \omega_j \frac{dq_j(\bar{t})}{d\bar{t}} + \omega_j^2 q_j(\bar{t}) = P_j(\bar{t}), \tag{12}$$

where the circular frequency of the beam $\omega_j = \beta_j^2$, the damping ratio of the mode $\zeta_j = \bar{a}/2\omega_j$, and the simplified expression of the right of Eq. (4) $P_j(\bar{t}) = [Y'_j(\bar{v}\bar{t}) - Y'_j(\bar{v}\bar{t} + \bar{b})]m(\bar{t})$, in which $Y'_j(\bar{v}\bar{t})$ and $Y'_j(\bar{v}\bar{t} + \bar{b})$ are the first derivatives of the modal function that depends on $\bar{x}$, when $\bar{x} = \bar{v}\bar{t}$ and $\bar{x} = \bar{v}\bar{t} + \bar{b}$.

TABLE I. Material properties and geometric parameters.

Parameter	Definition	Value	Unit
T_0	Thermal relaxation time	0.1	s
η_0	Light adsorption constant	0.00022	1/s
E	Young's modulus of beam	1	MPa
ν	Poisson ratio of beam	0.5	
ρ	Mass density of beam	1000	kg/m^3
a	Damping coefficient [61]	10000	kg/m^3
l	Beam length	0.01	m
h	Beam height	0.0001	m
C_0	Shrinkage coefficient [62–64]	0.2–0.7	
I_0	Light intensity	0–500	KW/m^2
d_0	Penetration depth	0.00001	m

Therefore, the Duhamel integral can be used to represent the solution to Eq. (12):

$$q_j(\bar{t}) = \frac{m(\bar{t})}{\omega_{dj}} \int_0^{\bar{t}} [Y'_j(\bar{v}\bar{\tau}) - Y'_j(\bar{v}\bar{\tau} + \bar{b})] \exp[-\varepsilon_j \omega_j(\bar{t} - \bar{\tau})]$$

$$\times \sin[\omega_{dj}(\bar{t} - \bar{\tau})] \sin(j\pi\bar{\tau}) d\bar{\tau}, \tag{13}$$

where the response frequency of this damped system, ω_{dj}, is $\omega_j \sqrt{1 - \zeta_j^2}$.

B. Solution method

To investigate the dynamic response of the LCE simply supported beam, we need to determine the typical values of the parameters. Material properties and geometric parameters, as well as the corresponding dimensionless parameters, are listed in Tables I and II, respectively. We will make use of the above typical system parameters in our following calculation. To calculate the dynamic response of the LCE simply supported beam under moving illumination, the integration for different times is used to calculate $q_j(\bar{t})$ in Eq. (13). Once $q_j(\bar{t})$ is solved, by multiplying the mode shape function $Y_j(\bar{x}) = \sin \beta_j \bar{x}$ with Eq. (10), we can obtain the dynamic response $W(\bar{x}, \bar{t})$ according to the modal superposition.

III. DYNAMIC DEFLECTION OF LCE SIMPLY SUPPORTED BEAM UNDER MOVING ILLUMINATION

According to the principle of modal superposition, there exist two independent variables, namely, time $\bar{t}$ and position $\bar{x}$, in the equation for dynamic deflection obtained by superposition. It is more convenient to set one independent variable as a fixed variable and then change the other independent variable so that we can simplify the three-dimensional curve of the dynamic response to a two-dimensional curve. In this way, as shown in Figs. 2 and 3, we can obtain the dynamic deflection of the beam at a fixed time and a fixed position, respectively, through setting the independent variables $\bar{t}$ and

TABLE II. Dimensionless parameters.

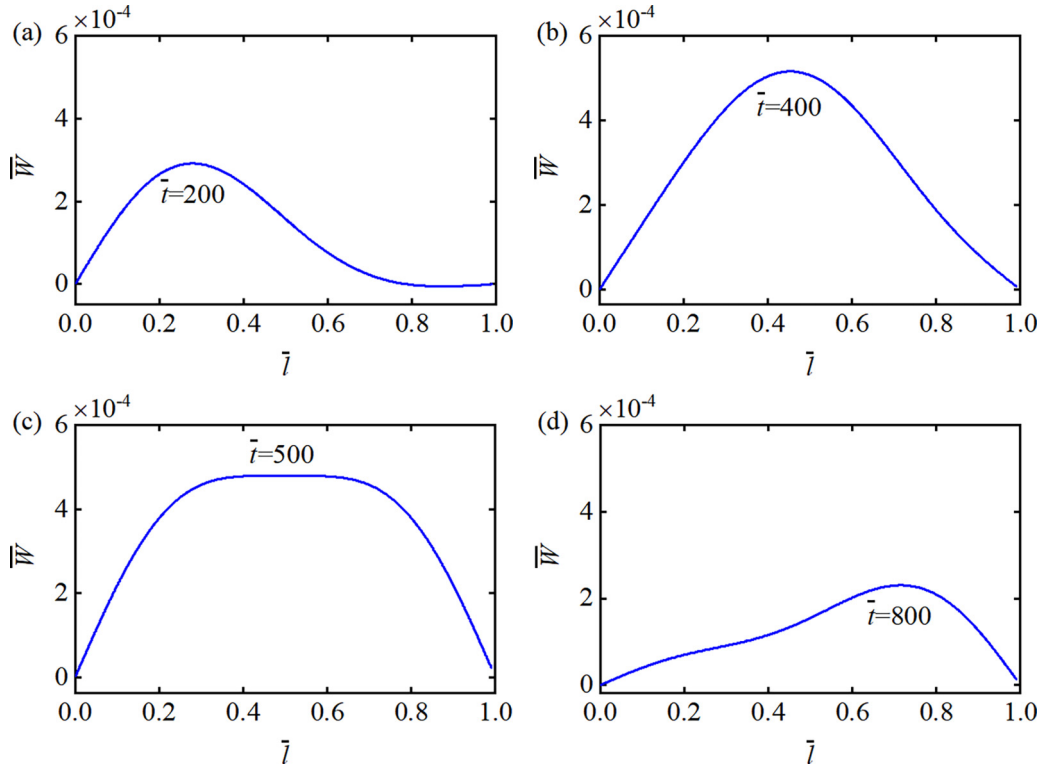| $\bar{I}_0$	C_0	$\bar{b}$	$\bar{a}$	$\bar{v}$
0–1	0.2–0.7	0.01–0.1	0–1	0–0.1

FIG. 2. The dynamic deflection of the beam at different time points under moving illumination: (a) $\bar{t} = 200$, (b) $\bar{t} = 400$, (c) $\bar{t} = 500$, and (d) $\bar{t} = 800$.

$\bar{x}$ as fixed variables, respectively. This is conducive to the theoretical study of the dynamic responses of the LCE simply supported beam under moving illumination.

Figure 2 depicts the dynamic deflections of the beam under moving illumination at different time points, with system parameters being set to $\bar{a} = 0.3$, $\bar{b} = 0.01$, $C_0 = 0.7$, $\bar{I}_0 = 0.8$, and $\bar{v} = 0.001$. Only the first three orders of the response mode are employed, as the influences of the higher-order frequencies on the structure are negligible. The peak of the dynamic deflection curve generally occurs at the illuminated position on the beam. As the illumination moves, so does the position where the peak appears, and the dynamic deflection curve of the entire beam is also changing. It is apparent that

the deflection of the beam is symmetric when the illumination reaches the nidpoint of the beam.

Figure 3 describes the dynamic deflections of the beam at different positions under moving illumination with the given parameters $\bar{a} = 0.3$, $\bar{b} = 0.01$, $C_0 = 0.7$, $\bar{I}_0 = 0.8$, and $\bar{v} = 0.001$. It is clear that the response curves of the beam at different positions are different under moving illumination. The curve peak occurs at the position where the illumination arrives. The mid-span is observed to possess the largest peak amplitude among all the portions of the beam. Consequently, it is more practical to choose the mid-span of a beam as the research object in the qualitative analysis of the LCE simply supported beams under moving illumination. The oscillation behavior of the curve is attributed to the fact that the frequency of the moving illumination is much smaller than the natural frequency of the beam, and the forced vibration of the beam is still accompanied by a certain amount of free vibration.
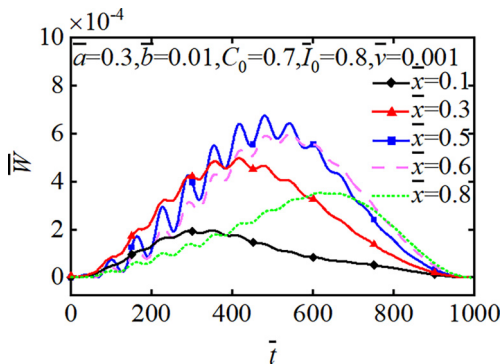
IV. PARAMETRIC ANALYSIS

The dynamic response under moving illumination plays an important role in LCE-based robots, actuators, and energy collectors, among which the simply supported beam is the simplest and most basic element. To explore the role of the dynamic response of the LCE beam on future applications, we calculate the dynamic responses of the simply supported beam under different factors, including the external parameters light intensity $\bar{I}_0$, illumination width $\bar{b}$, and moving speed of illumination, $\bar{v}$, and the driving parameters shrinkage coefficient C_0 and damping coefficient $\bar{a}$.

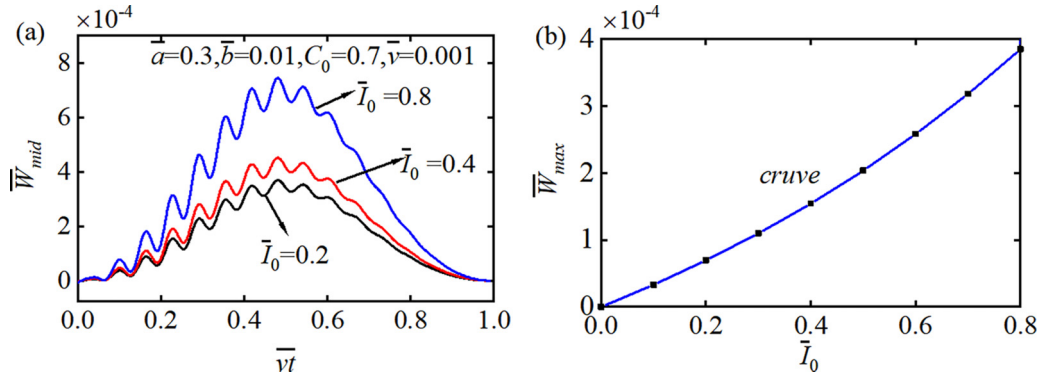FIG. 3. The dynamic deflection of the beam at different positions under moving illumination.

FIG. 4. The influence of light intensity on the dynamic response of the LCE simply supported beam. (a) The influence of light intensity on the mid-span deflection of the beam. (b) The variation of the maximum mid-span amplitude of the beam under different light intensity.

A. Influence of light intensity

Figure 4 illustrates how light intensity $\bar{I}_0$ influences the dynamic response of the beam, for $\bar{a} = 0.3$, $\bar{b} = 0.01$, $C_0 = 0.7$, and $\bar{v} = 0.001$. According to Fig. 4(a), the light intensity $\bar{I}_0$ has a great influence on the mid-span deflection of the beam when the other parameters are the same. The larger $\bar{I}_0$ is, the larger the response of the simply supported beam becomes. As $\bar{I}_0$ increases from 0.2 to 0.8, the mid-span deflection presents a significant increase. As can be seen in Fig. 4(b), the value of the maximum mid-span amplitude increases nonlinearly as light intensity $\bar{I}_0$ rises. In summary, with the increase of light intensity $\bar{I}_0$, the beam absorbs more energy from the illumination, and its response is also greater. Therefore, as one of the external parameters affecting the dynamic response of the system, the light intensity plays an important role in regulating it.

B. Influence of the illumination width

Figure 5 presents the influence of illumination width $\bar{b}$ on the dynamic response of the LCE simply supported beam, for $\bar{a} = 0.3$, $C_0 = 0.7$, $\bar{I}_0 = 0.8$, and $\bar{v} = 0.001$. Figure 5(a) demonstrates that the mid-span deflection of the beam increases as the illumination width $\bar{b}$ increases. The position of the peak value on the curve shifts slightly forward as the illumination width $\bar{b}$ increases. This is attributed to the fact

that the increase in illumination width reduces the time for the illumination to move to the mid-span of the beam. If we wish to obtain the peak amplitude in advance in practical engineering, the illumination width $\bar{b}$ can be adequately increased. Figure 5(b) depicts a nonlinear increase in the maximum mid-span amplitude of the beam as the illumination width $\bar{b}$ is increased. Hence, the adjustment of the illumination width $\bar{b}$ can change the amplitude and the moment of peak generation.

C. Influence of the moving speed of illumination

Figure 6 illustrates the influence of moving speed of illumination, $\bar{v}$, on the response of the LCE simply supported beam for $\bar{a} = 0.3$, $\bar{b} = 0.01$, $C_0 = 0.7$, and $\bar{I}_0 = 0.8$. As observed in Fig. 6(a), when $\bar{v} \leqslant 0.015$, the mid-span deflection of the beam increases as the moving speed of illumination, $\bar{v}$, increases. The dynamic response under $\bar{v} = 0.028$ is smaller than that under $\bar{v} = 0.015$. To accurately identify the moving speed of illumination, $\bar{v}$, that peaks the maximum mid-span amplitude of the beam, we expand the range of values for the speeds and reduce the interval between each speed in Fig. 6(b). As the moving speed of illumination increases, the maximum mid-span amplitude of the beam increases and then decreases. When $\bar{v} = 0.015$, the maximum mid-span amplitude of the beam reaches a peak. In general, the LCE simply supported beam exhibits an increased dynamic response when the moving speed of illumination is within a
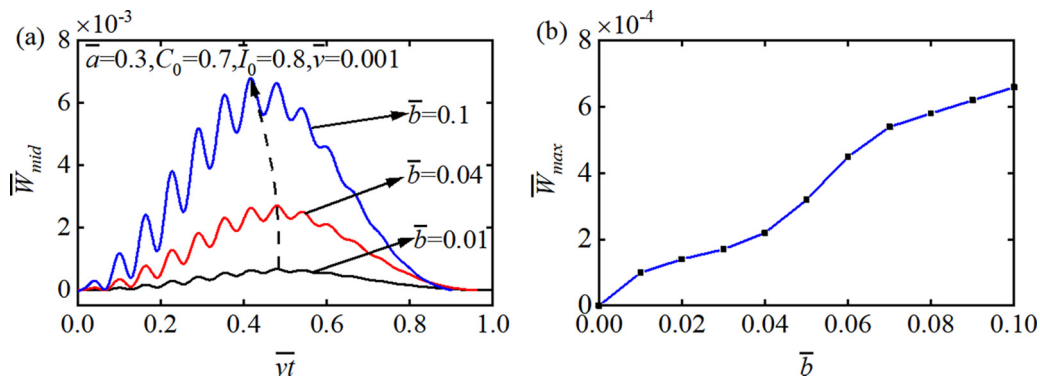

FIG. 5. The influence of illumination width on the dynamic response of the LCE simply supported beam. (a) The influence of illumination width on the mid-span deflection of the beam. (b) The variation of the maximum mid-span amplitude of the beam under different illumination widths.
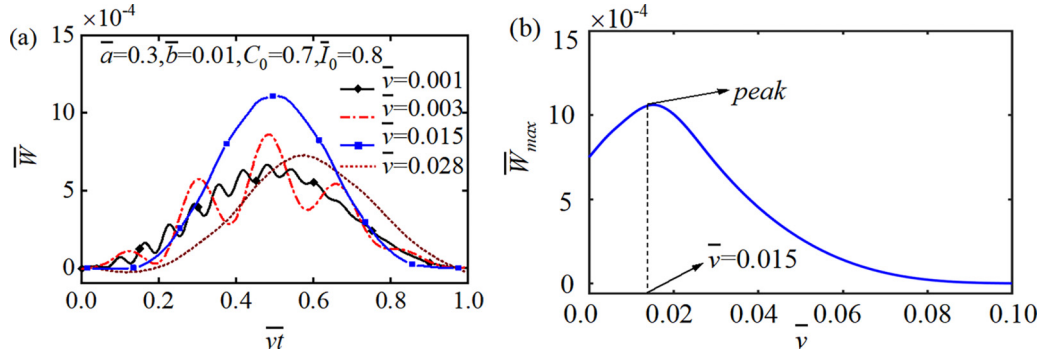
FIG. 6. The influence of moving speed of illumination on the dynamic response of the LCE simply supported beam. (a) The influence of moving speed of illumination on the mid-span deflection of the beam. (b) The variation of maximum mid-span amplitude of the beam under different moving speeds of illumination.

specific range. When this phenomenon occurs, the frequency of moving illumination approaches or equals the natural frequency of the LCE beam. The natural frequencies of the free response of simply supported beams, ω_{cr}, are as follows: $\omega_{cr_i} = (i\pi)^2 \sqrt{\frac{B}{\rho l^4}}$ ($i = 1, 2, 3, \ldots$) [69].

Converting the frequency into velocity, we can get the first-order critical velocity $\bar{v}_{cr_1} = 0.0167$, which corresponds to the first-order critical frequency. The result is almost consistent with the conclusion obtained according to Fig. 6. Therefore, it is concluded that the amplitude of the mid-span vibration response can be adjusted by changing the moving speed of illumination, and the amplitude of the mid-span vibration is the largest only when the velocity reaches the first-order critical velocity.

D. Influence of the shrinkage coefficient

Figure 7 depicts the influence of shrinkage coefficient C_0 on the dynamic response of the LCE simply supported beam, for $\bar{a} = 0.3$, $\bar{b} = 0.01$, $\bar{I}_0 = 0.7$, and $\bar{v} = 0.001$. Figure 7(a) shows that the mid-span deflection of the beam increases as the shrinkage coefficient C_0 increases. The reason is that the increase of the material shrinkage coefficient results in significant increase of the energy conversion medium, which further improves the efficiency of the energy conversion. As

shown in Fig. 7(b), the maximum mid-span amplitude of the beam increases linearly with the increase in the shrinkage coefficient C_0. Overall, the amplitude of the LCE beam can be adjusted by Eq. (5). The shrinkage coefficient C_0 can be examined in engineering applications to modify the response of the beam.

E. Influence of the damping coefficient

Figure 8 illustrates the influence of damping coefficient $\bar{a}$ on the dynamic response of the LCE beam, for $\bar{b} = 0.01$, $C_0 = 0.7$, $\bar{I}_0 = 0.8$, and $\bar{v} = 0.001$. Figure 8(a) presents that with the damping coefficient $\bar{a}$ increasing from 0.005 to 0.6, the mid-span deflection of the beam gradually decreases and the beam oscillation becomes stable. As illustrated in Fig. 8(b), with the increasing damping coefficient $\bar{a}$, the maximum mid-span amplitude of the beam gradually falls and then remains almost constant due to the excessive damping. In general, the increased damping is responsible for this phenomenon. In order to overcome the damping, the beam needs to consume more energy, which reduces the amplitude. Thus, through an appropriate variation of the damping coefficient, the amplitude of the dynamic response and the oscillation degree of the beam can be adjusted.
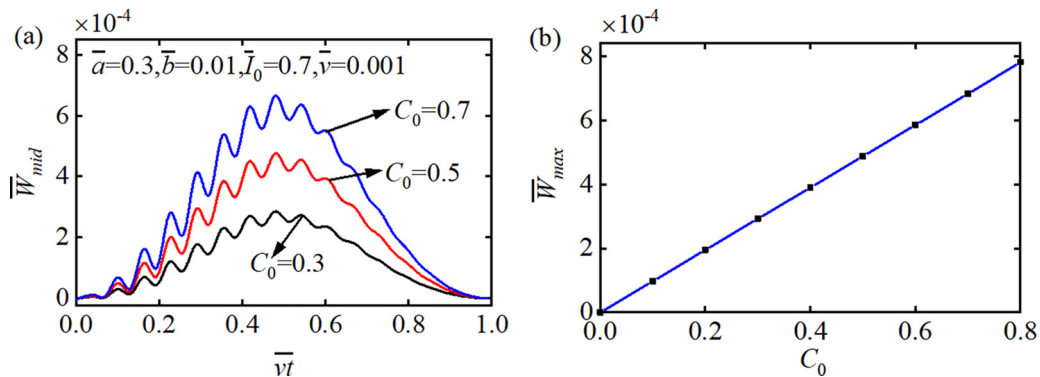

FIG. 7. The influence of shrinkage coefficient on the dynamic response of the LCE simply supported beam. (a) The influence of shrinkage coefficient on the mid-span deflection of the beam. (b) The variation of the maximum mid-span amplitude of the beam under different shrinkage coefficients.
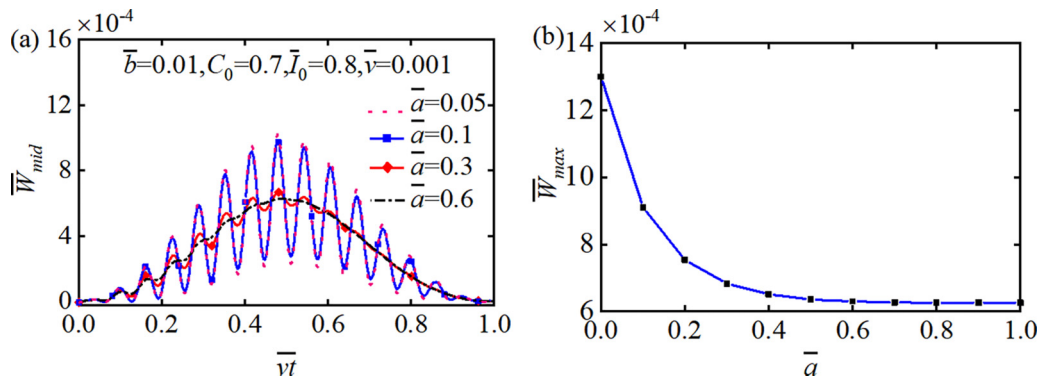
FIG. 8. The influence of damping coefficient on the dynamic response of the LCE simply supported beam. (a) The influence of damping coefficient on the mid-span deflection of the beam. (b) The variation of the maximum mid-span amplitude of the beam under different damping coefficients.

V. CONCLUSION

Light-powered LCE devices can be applied in a wide range of applications such as soft robots and microdrives, due to their advantages of remote controllability and simple structure. The dynamic response of LCE devices driven by moving illumination is rarely studied. In this paper, a nonlinear dynamic model of the simply supported LCE beam under moving illumination is established, and the analytical solution is derived using modal superposition and Duhamel integration. Under moving illumination, the LCE simply supported beam performs a forced response, converting light energy into mechanical energy, which is different from the conventional mechanically driven mode. The dynamic forced response of the LCE simply supported beam is systematically analyzed through theoretical formulations and numerical calculations. The dynamic response of the LCE simply supported beam under moving illumination, which is brought about by the coupling of optical deformation and its motion, is then illustrated, along with the methods for managing the system response.

In addition, the dependence of the dynamic response on five physical parameters is quantitatively given. The results demonstrate that when the moving speed of illumination reaches the first-order critical velocity, the maximum amplitude of the dynamic response at the beam mid-span peaks. Besides, the dynamic response of the LCE beam can be enhanced by increasing the illumination width, light intensity, and shrinkage coefficient or reducing the damping coefficient. To sum up, changing the internal parameters and driving parameters allows one to modify the dynamic response of the beam. In the next stage, it is worth further illustrating the dynamic response result by experimental verification to confirm the numerical calculation and explore its applications, and we expect that the current work has the potential to give rise to new and diverse design ideas for soft robotics, energy harvesters, micromachines, and so on.

ACKNOWLEDGMENTS

[1] Y. L. Yu, M. Nakano, and T. Ikeda, Photoinduced bending and unbending behavior of liquid-crystalline gels and elastomers, Pure Appl. Chem. **76**, 1467 (2004).

[2] T. J. White and D. J. Broer, Programmable and adaptive mechanics with liquid crystal polymer networks and elastomers, Nat. Mater. **14**, 1087 (2015).

[3] X. L. Pang, J. A. Lv, C. Y. Zhu, L. Qin, and Y. L. Yu, Photodeformable azobenzene-containing liquid crystal polymers and soft actuators, Adv. Mater. **31**, 1904224 (2019).

[4] L. Qin, X. J. Liu, and Y. L. Yu, Soft actuators of liquid crystal polymers fueled by light from ultraviolet to near infra-red, Adv. Opt. Mater. **9**, 2001743 (2021).

[5] W. Hu, G. Z. Lum, M. Mastrangeli, and M. Sitti, Small-scale soft-bodied robot with multimodal locomotion, Nature (London) **554**, 81 (2018).

[6] M. Vatankhah-Varnoosfaderani, W. F. Daniel, A. P. Zhushma, Q. Li, B. J. Morgan, and K. Matyjaszewski, Bottlebrush elastomers: A new platform for freestanding electroactuation, Adv. Mater. **29**, 201604209 (2017).

[7] H. Palza, P. A. Zapata, and C. Angulo-Pineda, Electroactive smart polymers for biomedical applications, Materials **12**, 277 (2019).

[8] P. J. Driest, D. J. Dijkstra, D. Stamatialis, and D. W. Grijpma, Tough combinatorial poly(urethane-isocyanurate) polymer networks and hydrogels synthesized by the trimerization of mixtures of NCO-prepolymers, Acta Biomater. **105**, 87 (2020).

[9] E. Zant and D. W. Grijpma, Synthetic biodegradable hydrogels with excellent mechanical properties and good cell adhesion characteristics obtained by the combinatorial synthesis

of photo-cross-linked networks, Biomacromolecules **17**, 1582 (2016).

[10] M. Grasinger, C. Majidi, and D. Kaushik, Nonlinear statistical mechanics drives intrinsic electrostriction and volumetric torque in polymer networks, Phys. Rev. E **103**, 042504 (2021).

[11] X. L. Zhuang, W. Zhang, K. M. Wang, Y. F. Gu, Y. W. An, and X. Q. Zhang, Active terahertz beam steering based on mechanical deformation of liquid crystal elastomer metasurface, Light Sci. Appl. **12**, 14 (2023).

[12] W. Lehmann, H. Skupin, C. Tolksdorf, E. Gebhard, R. Zental, and P. Kruger, Giant lateral electrostriction in ferroelectric liquid-crystalline elastomers, Nature (London) **410**, 447 (2001).

[13] Y. H. Na, Y. Aburaya, H. Orihara, and K. Hiraoka, Measurement of electrically induced shear strain in a chiral smectic liquid-crystal elastomer, Phys. Rev. E **83**, 061709 (2011).

[14] D. Corbett and M. Warner, Deformation and rotations of free nematic elastomers in response to electric fields, Soft Matter **5**, 1433 (2009).

[15] F. Atsushi, U. Kenji, K. Patrick, and T. Toshikazu, Electrically driven director-rotation of swollen nematic elastomers as revealed by polarized Fourier transform infrared spectroscopy, Phys. Rev. E **79**, 051702 (2009).

[16] C. M. Spillmann, J. Naciri, B. R. Ratna, R. L. Selinger, and J. V. Selinger, Electrically induced twist in smectic liquid-crystalline elastomers, J. Phys. Chem. B **120**, 6368 (2008).

[17] H. Zeng, O. M. Wani, P. Wasylczyk, R. Kaczmarek, and A. Priimagi, Self-regulating iris based on light-actuated liquid crystal elastomer, Adv. Mater. **29**, 1701814 (2017).

[18] K. Kumar, C. Knie, D. Bleger, M. A. Peletier, H. Friedrich, and H. Stefan, Chaotic self-oscillating sunlight-driven polymer actuator, Nat. Commun. **7**, 11975 (2016).

[19] O. M. Wani, H. Zeng, and A. Priimagi, A light-driven artificial flytrap, Nat. Commun. **8**, 15546 (2017).

[20] H. Zeng, O. M. Wani, P. Wasylczyk, and A. Priimagi, Light-driven, caterpillar-inspired miniature inching robot, Macromol. Rapid Commun. **39**, 10 (2018).

[21] A. Rešetič, J. Milavec, B. Zupančič, V. Domenici, and B. Zalar, Polymer-dispersed liquid crystal elastomers, Nat. Commun. **7**, 13140 (2016).

[22] N. Hama and U. Kenji, Thermal response of cholesteric liquid crystal elastomers, Phys. Rev. E **92**, 022501 (2015).

[23] D. Ge and K. Li, Pulsating self-snapping of a liquid crystal elastomer bilayer spherical shell under steady illumination, Int. J. Mol. Sci. **233**, 107646 (2022).

[24] J. M. Haberl, A. Sanchez-Ferrer, A. M. Mihut, H. Dietsch, A. M. Hirt, and R. Mezzenga, Liquid-crystalline elastomer-nanoparticle hybrids with reversible switch of magnetic memory, Adv. Mater. **25**, 1787 (2013).

[25] K. D. Harris, C. W. Bastiaansen, J. Lub, and D. J. Broer, Self-assembled polymer films for controlled agent-driven motion, Nano Lett. **5**, 1857 (2005).

[26] A. Petelin and M. Čopič, Strain dependence of the nematic fluctuation relaxation in liquid-crystal elastomers, Phys. Rev. E **82**, 011703 (2010).

[27] S. Palagi, A. G. Mark, S. Y. Reigh, K. Melde, T. Qiu, and H. Zeng, Structured light enables biomimetic swimming and versatile locomotion of photoresponsive soft microrobots, Nat. Mater. **15**, 647 (2016).

[28] M. A. Eddings, M. A. Johnson, and B. K. Gale, Determining the optimal PDMS-PDMS bonding technique for microfluidic devices, J. Micromech. Microeng. **18**, 067001 (2008).

[29] N. F. Lepora, P. Verschure, and T. J. Prescott, The state of the art in biomimetics, Bioinspir. Biomim. **8**, 013001 (2013).

[30] D. L. Thomsen, P. Keller, J. Naciri, R. Pink, H. Jeon, and D. Shenoy, Liquid crystal elastomers with mechanical properties of a muscle, Macromolecules **34**, 5868 (2001).

[31] H. Wermter and H. Finkelmann, Liquid crystalline elastomers as artificial muscles, e-Polym. **1**, 1 (2001).

[32] S. Petsch, A. Grewe, L. Köbele, S. Sinzinger, and H. Zappe, Ultrathin Alvarez lens system actuated by artificial muscles, Appl. Opt. **55**, 2718 (2016).

[33] M. H. Li and P. Keller, Artificial muscles based on liquid crystal elastomers, Philos. Trans. R. Soc. A **364**, 2763 (2006).

[34] T. Guin, B. A. Kowalski, R. Rao, A. D. Auguste, C. A. Grabowski, and P. F. Lloyd, Electrical control of shape in voxelated liquid crystalline polymer nanocomposites, ACS Appl. Mater. Interface **10**, 1187 (2018).

[35] S. Courty, J. Mine, A. R. Tajbakhsh, and E. M. Terentjev, Nematic elastomers with aligned carbon nanotubes: New electromechanical actuators, Europhys. Lett. **64**, 654 (2003).

[36] M. D. Hager, S. Bode, C. Weber, and U. S. Schubert, Shape memory polymers: Past, present and future developments, Prog. Polym. Sci. **49**, 3 (2015).

[37] Q. Zhao, H. J. Qi, and T. Xie, Recent progress in shape memory polymer: New behavior, enabling materials, and mechanistic understanding, Prog. Polym. Sci. **49**, 79 (2015).

[38] C. Ohm, M. Brehmer, and R. Zentel, Liquid crystalline elastomers as actuators and sensors, Adv. Mater. **22**, 3366 (2010).

[39] H. Kim, J. A. Lee, C. P. Ambulo, H. B. Lee, S. Kim, and V. V. Naik, Intelligently actuating liquid crystal elastomer-carbon nanotube composites, Adv. Funct. Mater. **29**, 1905063 (2019).

[40] N. J. Dawson, M. G. Kuzyk, J. Neal, P. Luchette, and P. Palffy-Muhoray, Cascading of liquid crystal elastomer photomechanical optical devices, Opt. Commun. **284**, 991 (2011).

[41] B. Firouzi and M. Zamanian, The effect of capillary and intermolecular forces on instability of the electrostatically actuated microbeam with T-shaped paddle in the presence of fringing field, Appl. Math. Modell. **71**, 243 (2019).

[42] I. Karimipour, Y. T. Beni, and A. H. Akbarzadeh, Size-dependent nonlinear forced response and dynamic stability of electrically actuated micro-plates, Commun. Nonlinear Sci. Numer. Simul. **78**, 104856 (2019).

[43] Z. Qin, F. Chu, and J. Zu, Free vibrations of cylindrical shells with arbitrary boundary conditions: A comparison study, Int. J. Mech. Sci. **133**, 91 (2017).

[44] Z. Qin, Z. Yang, F. Chu, and J. Zu, Free vibration analysis of rotating cylindrical shells coupled with moderately thick annular plates, Int. J. Mech. Sci. **142**, 127 (2018).

[45] H. A. Hajnayeb and S. E. Khadem, Nonlinear vibration and stability analysis of a double-walled carbon nanotube under electrostatic actuation, J. Sound Vib. **331**, 2443 (2012).

[46] Z. Qin, X. Pang, B. Safaei, and F. Chu, Free vibration analysis of rotating functionally graded CNT reinforced composite cylindrical shells with arbitrary boundary conditions, Compos. Struct. **220**, 847 (2019).

[47] S. Liu, K. Z. Huang, K. F. Wang, and B. L. Wang, Programmable deformation of liquid crystal elastomer plates subjected to concentrated light illumination, Mech. Mater. **175**, 104501 (2022).

[48] M. Warner, C. D. Modes, and D. Corbett, Suppression of curvature in nematic elastica, Proc. R. Soc. A **466**, 3561 (2010).

[49] S. Serak, N. Tabiryan, R. Vergara, T. J. White, R. A. Vaia, and T. J. Bunning, Liquid crystalline polymer cantilever oscillators fueled by light, Soft Matter **6**, 779 (2010).

[50] K. Li and S. Q. Cai, Modeling of light-driven bending response of a liquid crystal elastomer beam, J. Appl. Mech. **83**, 031009 (2015).

[51] M. K. Lee, M. L. Smith, H. Koerner, N. Tabiryan, R. A. Vaia, and T. J. Bunning, Flexural–torsional oscillation of glassy azobenzene liquid crystal polymer networks, Adv. Funct. Mater. **21**, 2913 (2011).

[52] N. Torras, K. E. Zinoviev, J. E. Marshall, E. M. Terentjev, and J. Esteve, Bending kinetics of a photo-actuating nematic elastomer cantilever, Appl. Phys. Lett. **99**, 254102 (2011).

[53] M. A. Parrany, Nonlinear light-induced response behavior of liquid crystal elastomer beam, Int. J. Mech. Sci. **136**, 179 (2018).

[54] A. Goriely, D. E. Moulton, and L. A. Mihai, A rod theory for liquid crystalline elastomers, J. Elast. **153**, 509 (2023).

[55] C. Ahn, X. Liang, and S. Cai, Bioinspired design of light-powered crawling, squeezing, and jumping untethered soft robot, Adv. Mater. Technol. **4**, 1900185 (2019).

[56] M. Rogóż, J. Haberko, and P. Wasylczyk, Light-driven linear inchworm motor based on liquid crystal elastomer actuators fabricated with rubbing overwriting, Materials **14**, 6688 (2021).

[57] M. Rogóż, Z. Dziekan, K. Dradrach, M. Zmyslony, P. Nalecz-Jawecki, and P. Grabowski, From light-powered motors, to micro-grippers, to crawling caterpillars, snails and beyond—light-responsive oriented polymers in action, Materials **15**, 8214 (2022).

[58] H. Guo, M. O. Saed, and E. M. Terentjev, Heliotracking device using liquid crystalline elastomer actuators, Adv. Mater. **6**, 2100681 (2021).

[59] M. Rogóż, H. Zeng, C. Xuan, D. S. Wiersma, and P. Wasylczyk, Light-driven soft robot mimics caterpillar locomotion in natural scale, Adv. Opt. Mater. **4**, 1689 (2016).

[60] T. Hayashikawa and N. Watanabe, Dynamic behavior of continuous beams with moving loads, J. Eng. Mech. Div. **107**, 229 (1981).

[61] Y. Wang, A. Dang, Z. Zhang, R. Yin, Y. Gao, L. Feng, and S. Yang, Repeatable and reprogrammable shapemorphing from photoresponsive gold nanorod/liquid crystalelastomers, Adv. Mater. **32**, 2004270 (2020).

[62] W. Hou, J. Wang, and J. A. Lv, Bioinspired liquid crystalline spinning enables scalable fabrication of high-performing fibrous artificial muscles, Adv. Mater. **35**, 2211800 (2023).

[63] T. Hessberger, L. Braun, and R. Zentel, Microfluidic synthesis of actuating microparticles from a thiol-ene based main-chain liquid crystalline elastomer, Polymers **8**, 410 (2016).

[64] C. Ohm, C. Serra, and R. Zentel, A continuous flow synthesis of micrometer-sized actuators from liquid crystalline elastomers, Adv. Mater. **21**, 4859 (2010).

[65] K. D. Hjelmstad, *Fundamentals of Structural Mechanics* (Springer Science and Business Media, 2007).

[66] P. M. Hogan, A. R. Tajbakhsh, and E. M. Terentjev, UV manipulation of order and macroscopic shape in nematic elastomers, Phys. Rev. E **65**, 041720 (2002).

[67] H. Finkelmann, E. Nishikawa, and G. G. Pereira, A new opto-mechanical effect in solids, Phys. Rev. Lett. **87**, 015501 (2001).

[68] L. Frýba, in *Vibration of Solids and Structures under Moving Loads*, Mechanics of Structural Systems Vol. 1 (Springer, Berlin, 1972), pp. 13–32.

[69] N. Rodrigo, On the natural frequencies of simply supported beams curved in mode shapes, J. Sound. Vib. **485**, 115597 (2020).